

# Effect of Slicing Parameters on the Light Transmittance of 3D-printed Polyethylene Terephthalate Glycol Products

Chen Wang,<sup>a,b,\*</sup> Jiahao Yu,<sup>a,b</sup> Minhan Jiang,<sup>a,b</sup> and Jingyao Li<sup>a,b</sup>

To manufacture 3D-printed polyethylene terephthalate glycol (PETG) products with excellent light transmittance performance, this study evaluated the principle of light transmission and the influencing factors of fused deposition methods (FDM) 3D-printed PETG products. This study explored the influence of different slicing parameters (layer height, extrusion rate, and printing speed) on the light transmittance of PETG products *via* a UV-visible spectrophotometer. The results showed that, in the range of 0.1 to 0.3 mm, the PETG specimens with 0.2 mm layer height had the best light transmittance performance; in the range of 100% to 120%; the PETG specimens with 110% extrusion rate had the best light transmittance performance; in the range of 20 to 40 mm/s printing speed, the PETG specimens with 40 mm/s printing speed had the best light transmittance performance. Comparison of image visibility showed that PETG products with layer height of 0.2 mm, extrusion rate of 110%, and printing speed of 40 mm/s had the best image visibility.

DOI: 10.15376/biores.19.1.500-509

*Keywords:* Slicing parameters; Fused deposition modeling; Polyethylene terephthalate glycol products; Light transmittance performance

*Contact information:* a: College of Furnishings and Industrial Design, Nanjing Forestry University, Nanjing 210037, China; b: Jiangsu Co-Innovation Center of Efficient Processing and Utilization of Forest Resources, Jiangsu, China; \*Corresponding author: 996869559@qq.com

## INTRODUCTION

Polyethylene terephthalate-1,4-cyclohexanedimethanol ester (PETG) is a non-crystalline co-polyester and a bio-based plastic that is recyclable, with good viscosity and weather resistance, as well as being non-toxic and environmentally friendly (Wang *et al.* 2019). PETG is the product of polymerisation of three monomers, namely, purified terephthalic acid (PTA), bio-based ethylene glycol (MEG), and 1,4-cyclohexanedimethanol (CHDM), formed by ester-exchange method. Among them, bio-based ethylene glycol is converted from sugar or other bio-based products from non-food resources as raw materials (Feng *et al.* 2022). Compared with petroleum-based ethylene glycol, bio-based ethylene glycol has the advantages of fewer process steps, high environmental friendliness, and high flexibility in raw material selection. In the production process of PETG plastics, a certain amount (30% to 40%) of bio-based ethylene glycol is replaced by CHDM, which can inhibit crystallization and form an amorphous polymer, thus giving PETG plastics a high light transmittance (around 90%). Therefore, PETG plastics are suitable for the manufacture of products with high requirements for light transmittance and are widely used in the production of transparent plastic sheets and cosmetic bottles (Mo *et al.* 2022).

The PETG filament is one of the few bio-based 3D printing consumables with high toughness, impact strength, that is basically odorless when printing, and exhibits excellent processing and moulding performances, with a broad application prospect in the field of 3D printing (Wang *et al.* 2020). In actual production, PETG products manufactured by conventional moulding methods, such as extrusion moulding, injection moulding, and blow moulding, usually have excellent light transmittance performance, whereas PETG products produced by the fused deposition method (FDM) of 3D printing process have poor light transmittance performance (Yang *et al.* 2022). This can be attributed to irregular refraction and scattering caused by the filling pattern and structural defects (bonding neck gaps and bubble cavities) inside the products. Relevant studies have shown that the most significant factors affecting the light transmittance performance of 3D printed PETG products are the densification, homogeneity, and thickness of the products (Ding *et al.* 2022). Densification refers to the compactness of the filament stack inside the product, homogeneity refers to the uniform consistency of the internal composition of the product, and thickness mainly affects the absorption of light (Huang *et al.* 2022).

In order to print PETG products with excellent light transmittance performance, special settings of slicing parameters are required. Therefore, this study summarizes the light transmission principle and influencing factors of FDM 3D printed PETG products, measures the transmittance of experimental samples using UV-visible spectrophotometer, and explores the influence of different slicing parameters (layer height, extrusion rate, and printing speed) on the light transmittance performance of PETG products. Finally, the image visibility of PETG products was analysed by combining with enlarged images, and the best combination of slicing parameters in terms of light transmittance and image visibility was summarized.

## EXPERIMENTAL

### Materials

The PETG filament (Transparent color, 1.75 mm diameter, Miracle 3D; Kunshan, China) was used for additive manufacturing by the FDM.

### Specimen Preparation

The slicing parameters, which are setup instructions for the 3D printing, mainly affect the internal filling pattern and structural defects of PETG products. To investigate the influence of the slicing parameters on the light transmittance performance of PETG products, Solidworks software (Dassault Systemes, Education Version 2016, Paris, France) was applied to design the thin-flake rectangular specimens (length size of 30 mm, thickness size of 1 mm, height size of 50 mm). The three slicing parameters that mainly affect the light transmittance were selected: layer height, extrusion rate, and printing speed. On this basis, nine groups of PETG specimens were prepared for evaluation (Feng *et al.* 2019).

A G-450 3D printer (XYZ printing, 0.4 mm nozzle diameter, Miracle 3D; Kunshan, China) was used for additive manufacturing by the fused deposition method. To avoid the hollow filling structure, the filling density in the slicing parameters was set to the maximum value (100%) during the slicing process; at the same time, to avoid the irregular refraction, the direction of the filling filament inside the specimen must be parallel to the direction of the long edge of the specimen's outer wall (Liu *et al.* 2020). The rest of the main slicing

parameters were set as follows: extruding temperature (230 °C), filling pattern (straight line), hot bed temperature (70 °C), and retraction speed (50 mm/s).

### Performance Test

A UV-visible spectrophotometer (U-3900, Hitachi; Tokyo, Japan) was used to test the transmittance at the center point of each group of PETG specimens, and the reference standard was ISO 26723 (2020).

An industrial flush-focus microscope (CL-MA-48M, Colomer; Guangzhou, China) was used to observe the enlarged view of the PETG specimens.

## PRINCIPLE ANALYSIS

### Structural Defects of PETG Products

Slicing is the process of converting a 3D model into a machining code according to specific parameters using software, and it is also one of the key links in the FDM 3D printing process flow. Under the regular slicing parameter settings, printing transparent PETG filament through the FDM process is often prone to given a white frosted appearance, which is caused by irregular refraction and scattering due to the filling pattern and structural defects inside the product, of which the main structural defects are the bonding neck gaps and bubble cavities (Yang *et al.* 2021). The bonding neck gap is shown in Fig. 1 (X-Y section).

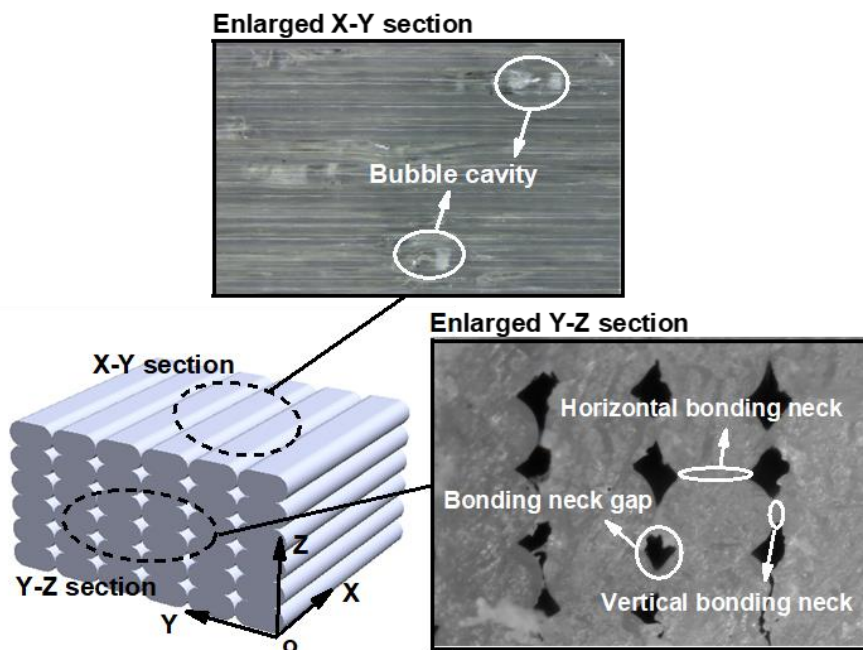


**Fig. 1.** Enlarged view of structural defects

The effect arises because the FDM process uses layer-by-layer stacking to generate the solid model, whereas the cross-section of the melted filament extruded from the print head has an elliptical shape. Under the pressure of the print head, the melted filament is infiltrated, diffused, and cross-linked with neighboring filament in the horizontal and

vertical direction to form the horizontal and vertical bonding neck structures (Wang *et al.* 2023). There is usually a gap between the horizontal and vertical bonding neck structures, which is called the bonding neck gap (Wang *et al.* 2022). In addition, there is a bubble cavity, as shown in Fig. 1 (Y-Z cross-section), the formation of bubble cavity is because the PETG filament has a strong water absorption, when the filament is heated and extruded in the print head, the water in the filament evaporates, forming bubbles. The air bubbles that cannot be eliminated remain inside the melted filament, and as the filament cools and deposits, bubble cavity defects are created (Liu *et al.* 2019).

### The Principle of Light Transmission of PETG Products

From the light transmission schematic (shown in Fig. 2), it can be seen that when the light passes through the 3D-printed PETG products, it first produces a small amount of diffuse reflection on the surface of the products. Most of the light is refracted at the air-polymer interface and enters into the interior of the PETG products. Within the internal structure of the products, which is dense and homogeneous, the light maintains a straight line propagation (shown in the light line a). When the light encounters the bonding neck gap or bubble cavity, due to the change of propagation medium, on the one hand, it causes the refraction of light, on the other hand, the secondary wave generated when the light encounters the inhomogeneous structure does not coincide with the direction of the main wave, and when the secondary wave is synthesized with the main wave, interference occurs, causing the scattering phenomenon. Scattering leads to a weakening of the intensity of the transmitted light and a reduction in the light transmittance of the PETG products (shown in lines b and c).

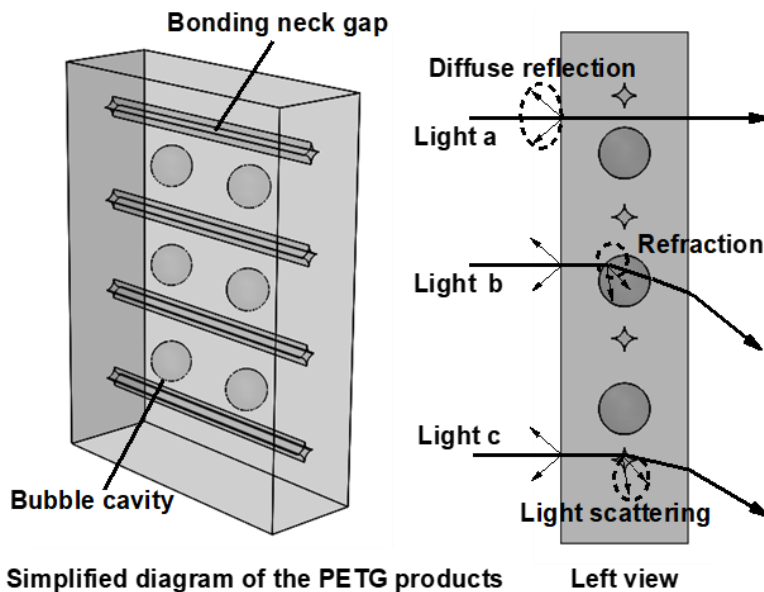


Fig. 2. Schematic diagram of light transmission

## RESULTS AND DISCUSSION

### Effect of Layer Height on Light Transmittance of PETG Products

The layer height is the thickness of each layer of filament when printing products (Li *et al.* 2022). The transmittance of PETG specimens with 0.1 mm, 0.2 mm, and 0.3 mm layer height was tested, and from the transmittance curves (Fig. 3), it can be seen that in the visible spectral region of 400 to 760 nm wavelengths, the light transmittance of the 0.2 mm layer height specimen achieved the best performance, the light transmittance of the 0.3 mm layer height was in the middle, and the transmittance of 0.1 mm layer height had the worst performance. The layer height affects the densification and thickness of PETG specimens, and as the layer height decreases, the molten filament material is extruded in the vertical direction (Z-axis direction) and expands in the horizontal direction (X-Y plane direction). Horizontal expansion on the one hand fills the bonding neck gaps, and on the other hand increases the thickness of the specimens. The PETG specimens with 0.3 mm layer height had bonding neck gaps inside, the densification was poor, and the light scattering was caused by the light passing through the bonding neck gaps, which reduces the light transmittance. The layer height of 0.1 mm increased the densification of the specimens, but it also increased the thickness, and the light absorption phenomenon increased, which also reduced the light transmittance. The layer height of 0.2 mm was just right to fill the bonding neck gaps, but it did not have an impact on the thickness. Therefore, in the range of 0.1 mm to 0.3 mm, the PETG specimens with 0.2 mm layer height exhibited the best light transmittance performance.

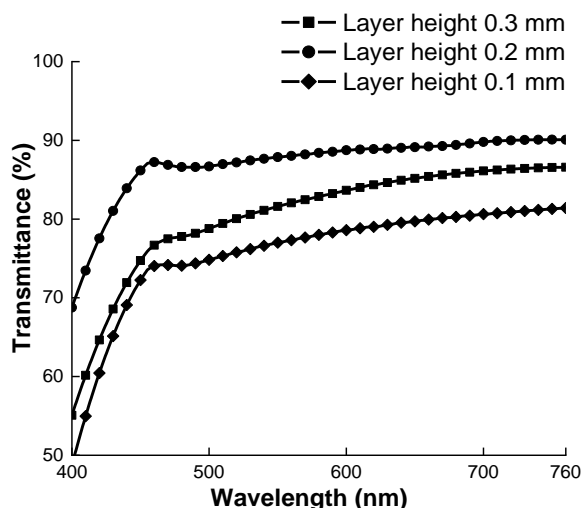


Fig. 3. Transmittance curves

### Effect of Extrusion Rate on Light Transmittance of PETG Products

Extrusion rate is the actual extruded amount of molten filament material. The light transmittances of PETG specimens with 100%, 110%, and 120% extrusion rate were tested. The transmittance curves in Fig. 4 show that in the visible spectral region of 400 to 760 nm, the light transmittance of 110% extrusion rate had the best performance, the 100% extrusion rate was in the middle, and the light transmittance of 120% extrusion rate had the worst performance. This is because the PETG specimens had internal bonding neck gaps at 100% extrusion rate, and the light passing through the bonding neck gaps triggered

scattering, which led to the weakening of the intensity of the transmitted light and a decrease in the transmittance of the specimen. By appropriately increasing the extrusion rate (110%), the actual extrusion of molten filaments in the print head was increased by approximately 10%, and these materials effectively filled the bonding neck gaps, increasing the densification and improving the light transmittance (Li *et al.* 2020). However, further increasing the extrusion rate (120%) will lead to the expansion of the specimen in the horizontal direction (X-Y plane direction), so that its thickness increases, and the optical range grows, and the light absorption phenomenon increases, and the light transmittance performance decreases instead (Liu *et al.* 2021). In conclusion, in the range of 100% to 120% extrusion rate, the PETG specimens with 110% extrusion rate have better densification and thickness, and the best light transmittance performance.

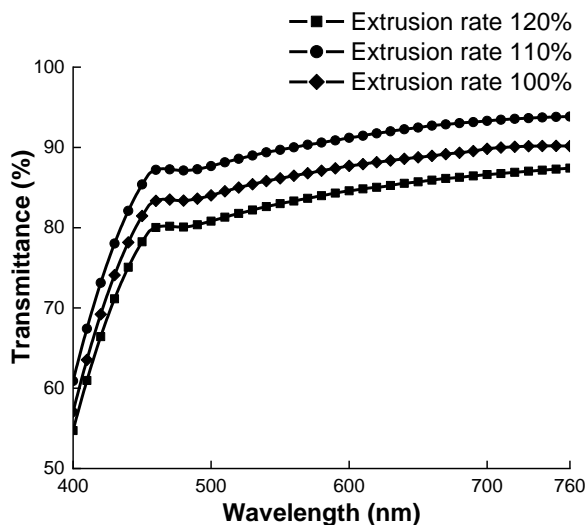


Fig. 4. Transmittance curves

### Effect of Printing Speed on Light Transmittance of PETG Products

The printing speed is the horizontal travelling speed of the print head. The light transmittance of PETG specimens was tested at 20, 30, and 40 mm/s printing speeds. From the transmittance curves, Fig. 5 shows that within the visible spectral region of 400 to 760 nm, the light transmittance of PETG specimens decreased as the printing speed decreased. Matching with the horizontal moving speed of the print head is the extrusion speed of the fused filament, and a slower moving speed of the print head results in a slower extrusion speed of the fused filament (Qi *et al.* 2019).

Because PETG material is highly absorbent, the slower the filament extrusion speed, the longer the heating time of the filament in the extrusion chamber. The water in the filament material is volatilized by heat to produce bubbles, which remain inside the deposited filament material, forming a bubble cavity, thus changing the homogeneity of the specimen's structure, causing the scattering of light, and reducing the light transmittance (Zhou and Xu 2022). In summary, in the range of 20 mm/s to 40 mm/s printing speed, the PETG specimens with 40 mm/s printing speed developed the lowest number of residual bubbles, better structural homogeneity, and the best light transmittance performance.

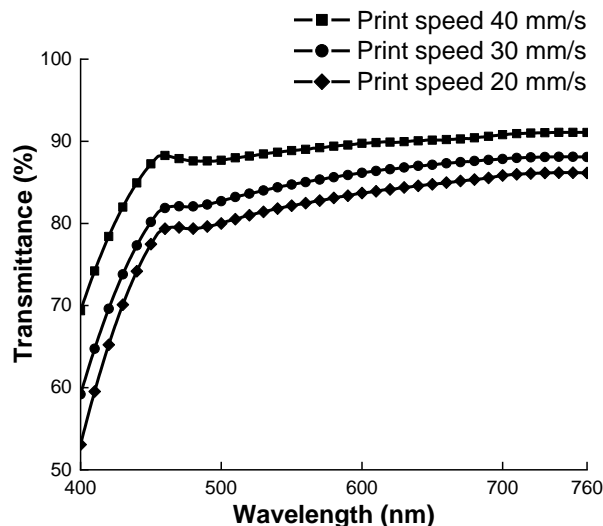


Fig. 5. Transmittance curves

### Comparison of Image Visibility of PETG Products

The image visibility can intuitively show the light transmittance performance of the object (Qi *et al.* 2023). For the three kinds of slicing parameters studied above, seven groups of PETG specimens were printed, and the PETG specimens were placed on top of white paper printed with the characters “3D”. The image visibility, when viewed through the PETG specimens, was observed by means of an industrial flush-focus microscope (Fig. 6). The slicing parameters of the reference group were a layer height of 0.2 mm, extrusion rate of 110%, and printing speed of 40 mm/s. These were the optimal light transmittance parameters obtained from the above experiments; the slicing parameters of the control group A were layer height of 0.1 mm or 0.3 mm, extrusion rate of 110%, and printing speed of 40 mm/s, which were used to compare the image visibility of PETG specimens under different layer heights; the slicing parameters of control group B were layer height of 0.2 mm, extrusion rate of 120% or 100%, and printing speed of 40 mm/s, which are used to compare the image visibility of PETG specimens under different extrusion rate; and the slicing parameters of control group C were layer height of 0.2 mm, extrusion rate of 110%, and printing speed of 20 or 30 mm/s, which are used to compare the image visibility of PETG specimens under different printing speeds.

Comparing the reference group and control group A, PETG specimens with 0.2 mm layer height appeared more transparent than the PETG specimens with 0.1 mm and 0.3 mm layer height, and the characters were displayed more clearly. The image visibility was better, which verifies the experimental conclusion above that the 0.2 mm layer height had the best light transmittance performance. Comparing the reference group and control group B, PETG specimens with 110% extrusion rate appeared more transparent than those with 120% and 100% extrusion rate, and the “3D” characters were displayed more vividly. These observations verified the conclusion of the above experiments, that is, that the 110% extrusion rate had the best light transmittance performance. Comparing the reference group and control group C, the bubble cavity inside the PETG specimens at 40 mm/s printing speed was clearly reduced, and there were fewer impurities around the “3D” character, which leads to better image visibility, and thus the light transmittance performance is better at 40 mm/s printing speed. In summary, the light transmittance performance and image

visibility of PETG products was best under the combination of slicing parameters of layer height at 0.2 mm, extrusion rate of 110%, and printing speed of 40 mm/s.

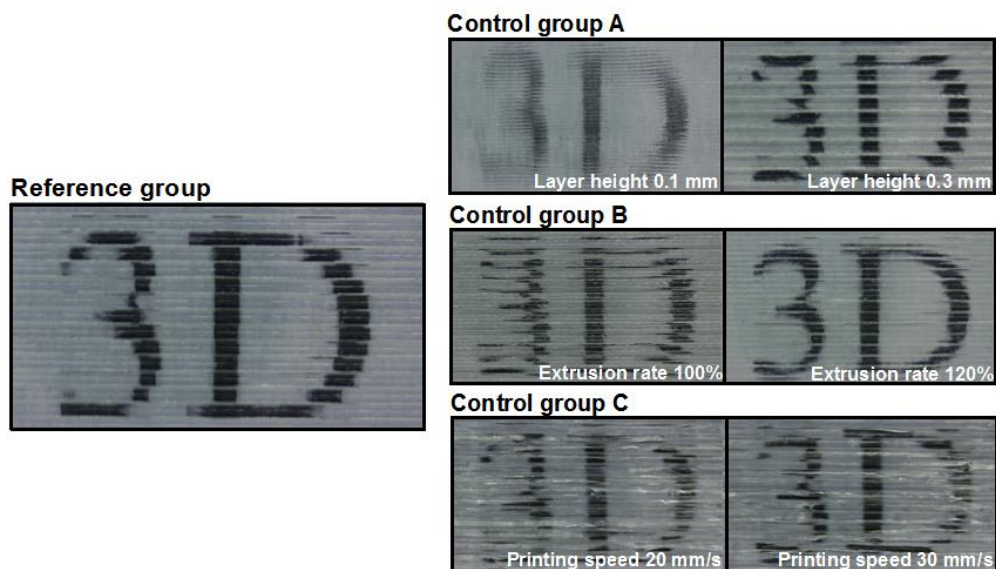


Fig. 6. Image visibility of PETG products

## POSSIBLE FUTURE WORK

With the continuous development of 3D printing technology, cellulose and its derivatives have been gradually applied to the preparation of 3D printing materials and the improvement or enhancement of the performance of printed products (Han *et al.* 2022). In this study, the light transmittance of 3D printed PETG products was investigated from the perspective of slicing parameters, and it is hoped that this research idea will be extended to cellulose-based 3D printing materials. A goal of such work would be to analyse the light transmittance of cellulose-based 3D printed products and achieve the improvement of the light transmittance of cellulose-based 3D printed products by optimising the slicing parameters.

## CONCLUSIONS

1. In the range of 0.1 to 0.3 mm layer height, the polyethylene terephthalate-1,4-cyclohexanedimethanol ester (PETG) specimens with 0.2 mm layer height were found to fill the bonding neck gaps without affecting the thickness of the products. Those conditions led to the best light transmittance performance. Within the range of 100% to 120% extrusion rates, the PETG specimens with 110% rate showed greater densification and thickness, and the best light transmittance performance; in the range of 20 to 40 mm/s printing speed, the PETG specimens with 40 mm/s exhibited the lowest number of residual bubbles, better homogeneity of the structure, and the best light transmittance performance.



2. Comparing the reference group and control group A, the image visibility of PETG specimens was better under 0.2 mm layer height; comparing the reference group and control group B, the image visibility of PETG specimens was better under 110% extrusion rate; comparing the reference group and control group C, the image visibility of PETG specimens was better under 40 mm/s printing speed. In conclusion, the light transmittance performance and image visibility of PETG specimens with the combination of layer height of 0.2 mm, extrusion rate of 110%, and printing speed of 40 mm/s was the best.

## REFERENCES CITED

- Ding, T.-T., Yan, X.-X., and Zhao, W.-T. (2022). "Effect of urea-formaldehyde resin-coated colour-change powder microcapsules on performance of waterborne coatings for wood surfaces," *Coatings* 12(9), article 1289. DOI: 10.3390/coatings12091289
- Feng, X.-H., Wu, Z.-H., Sang, R.-J., Wang, F., Zhu, Y.-Y., and Wu, M.-J. (2019). "Surface design of wood-based board to imitate wood texture using 3D printing technology," *BioResources* 14(4), 8196-8211. DOI: 10.15376/biores.14.4.8196-8211
- Feng, X.-H., Yang, Z.-Z., Wang, S.-Q., and Wu, Z.-H. (2022). "The reinforcing effect of lignin-containing cellulose nanofibrils in the methacrylate composites produced by stereolithography," *Polymer Engineering and Science* 2022(9), 2968-2976. DOI: 10.1002/pen.26077
- Han, Y., Yan, X.-X., and Zhao, W.-T. (2022). "Effect of thermochromic and photochromic microcapsules on the surface coating properties for metal substrates," *Coatings* 12(11), article 1642. DOI: 10.3390/coatings12111642
- Huang, N., Yan, X.-X., and Zhao, W.-T. (2022). "Influence of photochromic microcapsules on properties of waterborne coating on wood and metal substrates," *Coatings* 12(11), article 1750. DOI: 10.3390/coatings12121857
- ISO 26723 (2020). "Plastics – Determination of total luminous transmittance and reflectance," International Organization for Standardization, Geneva, Switzerland.
- Li, R.-R., Chen, J.-J., and Wang, X.-D. (2020). "Prediction of the color variation of moso bamboo during CO<sub>2</sub> laser thermal modification," *BioResources* 15(3), 5049-5057. DOI: 10.15376/biores.15.3.5049-5057
- Li, W.-B., Yan, X.-X., and Zhao, W.-T. (2022). "Preparation of crystal violet lactone complex and its effect on discoloration of metal surface coating," *Polymers* 14(20), article 4443. DOI: 10.3390/polym14204443
- Liu, X.-Y., Lv, M.-Q., Liu, M., and Lv, J.-F. (2019). "Repeated humidity cycling's effect on physical properties of three kinds of wood-based panels," *BioResources* 14(4), 9444-9453. DOI: 10.15376/biores.14.4.9444-9453
- Liu, Y., Hu, J., and Wu, Z.-H. (2020). "Fabrication of coatings with structural color on a wood surface," *Coatings* 10(1), article 32. DOI: 10.3390/coatings10010032
- Liu, Q., Gu, Y., Xu, W., Lu, T., Li, W., and Fan, H. (2021). "Compressive properties of green velvet material used in mattress bedding," *Applied Sciences* 11(23), article 11159. DOI:10.3390/app112311159
- Mo, X.-F., Zhang, X.-H., Fang, L., and Zhang, Y. (2022). "Research progress of wood-based panels made of thermoplastics as wood adhesives," *Polymers* 14(1), article 98. DOI: 10.3390/polym14010098

- Qi, Y.-Q., Shen, L.-M., Zhang, J.-L., Yao, J., Lu, R., and Miyakoshi, T. (2019). "Species and release characteristics of VOCs in furniture coating process," *Environmental Pollution* 2019(245), 810-819. DOI: 10.1016/j.envpol.2018.11.057
- Qi, Y.-Q., Sun, Y., Zhou, Z.-W., Huang, Y., Li, J.-X., and Liu, G.-Y. (2023). "Response surface optimization based on freeze-thaw cycle pretreatment of poplar wood dyeing effect," *Wood Research* 68(2), 293-305. DOI: 10.37763/wr.1336-4561/68.2.293305
- Wang, X.-H., Wu, Y., Chen, H., Zhou, X.-Y., Zhang, Z.-K., and Xu, W. (2019). "Effect of surface carbonization on mechanical properties of LVL," *BioResources* 14(1), 453-463. DOI: 10.15376/biores.14.1.453-463
- Wang, S., Chen, L., Xu, L.-J., Guan, H., Yan, S., and Wu, Z.-H. (2020). "Comparative study on the tensile performance of box frames constructed by keyed joints and dovetail joints," *BioResources* 15(4), 9291-9302. DOI: 10.15376/biores.15.4.9291-9302
- Wang, L., Han, Y., and Yan, X.-X. (2022). "Effects of adding methods of fluorane microcapsules and shellac resin microcapsules on the preparation and properties of bifunctional waterborne coatings for basswood," *Polymers* 14(18), article 3919. DOI: 10.3390/polym14183919
- Wang, Q., Feng, X.-H., and Liu, X.-Y. (2023). "Functionalization of nanocellulose using atom transfer radical polymerization and applications: A review," *Cellulose* 30, 8495-8537. DOI: 10.1007/s10570-023-05403-5
- Yang, L., Han, T.-Q., Liu, Y.-X., and Yin, Q. (2021). "Effects of vacuum heat treatment and wax impregnation on the color of *Pterocarpus macrocarpus* Kurz," *BioResources* 16(1), 954-963. DOI: 10.15376/biores.16.1.954-963
- Yang, Z.-Z., Feng, X.-H., Xu, M., and Rodrigue, D. (2022). "Printability and properties of 3D printed poplar fiber/polylactic acid biocomposites," *BioResources* 16(2), 2774-2788. DOI: 10.15376/biores.16.2.2774-2788
- Zhou, J.-C., and Xu, W. (2022). "Toward interface optimization of transparent wood with wood color and texture by silane coupling agent," *Journal of Materials Science* 57(10), 5825-5838. DOI: 10.1007/s10853-022-06974-7

Article submitted: October 17, 2023; Peer review completed: November 11, 2023;  
Revised version received and accepted: November 14, 2023; Published: November 21, 2023.

DOI: 10.15376/biores.19.1.500-509